

## Relaxation of the transport critical current in high- $T_c$ polycrystals

E. Altshuler and R. Cobas

*Superconductivity Laboratory, IMRE–Physics Faculty, University of Havana, 10400 La Habana, Cuba*

A. J. Batista-Leyva

*Superconductivity Laboratory, IMRE–Physics Faculty, University of Havana, 10400 La Habana, Cuba  
and Department of Physics, Engineering Faculty, University of Holguín, 80100 Holguín, Cuba*

C. Noda, L. E. Flores, and C. Martínez

*Superconductivity Laboratory, IMRE–Physics Faculty, University of Havana, 10400 La Habana, Cuba*

M. T. D. Orlando

*Group of New Materials, Brazilian Center of Physics Research, 22290-180 Rio de Janeiro, Brazil  
and Department of Physics, Universidade Federal do Espírito Santo, 29060-900 Espírito Santo, Brazil*

(Received 3 December 1998; revised manuscript received 9 February 1999)

We perform a systematic study of the time evolution of the transport critical current in polycrystalline samples of the high temperature superconducting system  $(\text{Hg}_{1-x}\text{Re}_x)\text{Ba}_2\text{Ca}_2\text{Cu}_3\text{O}_{8+\delta}$  and  $\text{YBa}_2\text{Cu}_3\text{O}_{7-\delta}$  after application and removal of an external magnetic field  $H_m$ . Within our time, temperature, and remanent field windows, the transport critical current increases logarithmically in time. The relaxation rates in the range 80–115 K decrease with increasing temperature at a fixed  $H_m$ , while temperature-dependent maxima are observed in the relaxation rate versus  $H_m$  plots. These experimental results are reproduced by a phenomenological model applicable to any high- $T_c$  polycrystals. In the model, the time increase of the transport current is determined by the effective field at the intergrain junctions, which relaxes in time due to the flux creep of the intragrain magnetization. [S0163-1829(99)00729-8]

### I. INTRODUCTION

Since the discovery of high- $T_c$  superconductors,<sup>1</sup> their relatively high rates of flux creep immediately captured the attention of researchers. In fact, the term “giant flux creep” was rapidly popularized after Yeshurun and Malozemoff’s 1988 pioneering paper.<sup>2</sup> Up to date, a vast majority of experimental work in the subject has focused on YBCO powders, polycrystals, crystals, and films,<sup>3</sup> in contrast with other materials with higher critical temperature such as BSCCO (Ref. 4) and TBCCO (Ref. 5). The HgBCCO system remains as the least studied high- $T_c$  superconductor from the point of view of thermally activated relaxation.<sup>6</sup>

Although most of the experimental and theoretical efforts on the subject have concentrated on the study of the relaxation of the *magnetization* of high- $T_c$  crystals, polycrystals, and films,<sup>3</sup> flux creep effects can also influence the time evolution of other measurable magnitudes of potential practical importance, such as the voltage associated with a constant transport current measured on a sample after the application of some magnetic field history.<sup>7–9</sup> This can be interpreted, at least in the case of polycrystals, as a consequence of the flux creep of grains magnetization which, in turn, affects the effective magnetic field at the intergranular weak links, thus influencing the transport properties of the sample. Even when these kind of experiments bring a unique local perspective of the relaxation of the grains into a polycrystal, unreachable from conventional magnetometric measurements, they have not covered a range of temperatures. Closely connected to these measurements are the brief reports by

Zhukov *et al.* in 1992 (Ref. 10) and by Ries *et al.* in 1994 (Ref. 11) on the relaxation at fixed temperatures and very limited magnetic field histories of YBCO polycrystals and of BSCCO-Ag tapes, respectively.

In this paper, we study *the time evolution of the transport critical current* of  $(\text{Hg}_{1-x}\text{Re}_x)\text{Ba}_2\text{Ca}_2\text{Cu}_3\text{O}_{8+\delta}$  and  $\text{YBa}_2\text{Cu}_3\text{O}_{7-\delta}$  polycrystals submitted to a variety of magnetic field histories and temperatures both experimentally and with the help of a phenomenological model which assumes an interpolation formula from collective creep theory<sup>12</sup> for the relaxation of the diamagnetic critical currents of the grains. Our measurements are performed using a PI controller which allows us to measure thousands of values of the transport critical current per hour. Within our time, temperature, and trapped field windows all the relaxations are nearly logarithmic, while the temperature and trapped field dependences of the relaxation rates are consistent with the results of our phenomenological model.

### II. EXPERIMENT

For the obtainment of HBCCO polycrystals, high-purity  $\text{BaCO}_3$ ,  $\text{CaCO}_3$ ,  $\text{CuO}$ ,  $\text{ReO}_2$ , and  $\text{HgO}$  powders were weighted to obtain the nominal composition  $(\text{Hg}_{1-x}\text{Re}_x)\text{Ba}_2\text{Ca}_2\text{Cu}_3\text{O}_{8+\delta}$ . The first four components were homogenized and heated at 850 °C for 12h in oxygen flow. After pelletization at 1 GPa, the pellets were calcined twice at 930 °C for 15 h in oxygen flow, with crushing be-

tween heat treatments. Then, they were submitted to 930 °C for 12 h in a flow of 20% oxygen and 80% argon. After this, HgO was added to the crushed pellets, and the mixture pelletized at 1 GPa in vacuum. The resulting compacts were introduced into a gold foil and then into a 8-mm-inner-diam quartz tube along with a ceramic material in order to obtain a filling factor of 1.1 g/cm<sup>3</sup>.<sup>13,14</sup> The quartz tube was sealed at 10<sup>-2</sup> Torr and introduced into an isostatic pressure furnace with 40 bars of argon. The temperature was raised to 700 °C at 300 °C/h, and then to 850 °C at 120 °C/h. The latter temperature was maintained for 15 h, and the sample cooled to room temperature at 120 °C/h.

For the obtention of the YBCO polycrystals, the standard ceramic procedure was used.<sup>15</sup> High-purity BaCO<sub>3</sub>, CuO, and Y<sub>2</sub>O<sub>3</sub> powders were weighted to obtain the nominal composition YBa<sub>2</sub>Cu<sub>3</sub>O<sub>7-δ</sub> and mixed. Successive calcinations were applied in air at 900, 920, and 940 °C for 16 h each, with crushing between treatments. After a final 2-h milling, the powders were pressed at 0.3G Pa. The resulting pellets were sintered at 950 °C for 16 h in air with heating and cooling rates of 1 °C/min.

From both kinds of samples, 10×0.7×0.7 mm<sup>3</sup> bars were cut from the pellets, to which four contacts were attached with silver paint in the standard four-probe arrangement. The two voltage contacts were 3 mm apart.

The critical current measurements were performed with a special PI pulsed-current setup.<sup>16</sup> A sequence of alternate current pulses with ON/OFF periods of 0.13 and 2.7 ms, respectively, is injected into the sample through the outer contacts, and a PI system dynamically adjusts the height of the pulses in order to keep a constant dissipation of 1 μV between the inner contacts (the voltage is sampled only at the horizontal current plateau at the top of each ON period). Then, the critical current at any applied field, temperature, or time is measured just by reading the corresponding bias current. In all cases, the temperature was controlled within ±0.01 K, and the magnetic field was applied using a copper solenoid within ±0.3 Oe. Three types of measurements were performed using this setup, in order of complexity.

(a) *Transport critical current versus temperature.* The critical current is measured at zero applied field while the temperature is decreased from 130 to 80 K at a rate of 2 K/min.

(b) *Transport flux trapping.* After erasing any previous magnetic history of the sample by increasing the temperature to 1.3 *T<sub>c</sub>* at zero field, the temperature is stabilized to the measurement value, and the magnetic field is increased at a rate of 20 Oe/s to a value *H<sub>m</sub>* and then suppressed at the same rate. Then, the critical current was measured. Special care was taken to guarantee a true zero-field cooling (ZFC) of the sample, within the limits imposed by the lack of shielding for Earth's magnetic field. The process is repeated for different values of *H<sub>m</sub>*, resulting in a *I<sub>c</sub>(H<sub>m</sub>, T, t* ≈ 10 s) versus *H<sub>m</sub>* curve.<sup>15</sup>

(c) *Transport critical current relaxation.* After erasing any previous magnetic history of the sample by increasing the temperature to 1.3*T<sub>c</sub>* at zero field, the temperature is stabilized to the measurement value, and the magnetic field is increased at a rate of 20 Oe/s to a value *H<sub>m</sub>* and then suppressed at the same rate. Special care was taken to guarantee a true zero-field cooling of the sample, within the lim-

its imposed by the lack of shielding for Earth's magnetic field. Then, the transport critical current is measured every second during 1 h, resulting in a *I<sub>c</sub>(H<sub>m</sub>, T, t)* versus *t* curve. The process is repeated for different values of *H<sub>m</sub>* and *T*.

### III. PHENOMENOLOGICAL MODEL

A well accepted model to estimate the increasing-field dependence of the transport critical current of a polycrystalline high-*T<sub>c</sub>* superconductor was early proposed by Peterson and Ekin in 1988.<sup>17</sup> It assumes that the intergrain weak links of the material can be regarded as a parallel network of superconducting-insulating-superconducting (SIS) Josephson junctions with a statistical distribution of junctions widths submitted to the applied field. In 1993, Altshuler *et al.*<sup>18</sup> and Müller and Matthews<sup>19</sup> further extended the model, introducing the possibility of calculating the transport critical current at a given field after *any* magnetic field history. The essence of their approach is to consider the junctions embedded into an effective magnetic field *H<sub>eff</sub>* resulting from the “competition” between the external field and the field associated with the magnetization of the superconducting grains. The grains are supposed to follow Bean's critical state model<sup>20</sup> conveniently modified to take into account their first critical field *H<sub>c1g</sub>*. The resulting critical current is a function of the maximum applied field *H<sub>m</sub>*, the temperature *T*, and the time elapsed since the magnetic field was suppressed, *t*. It can be written as

$$I_c(H_m, T, t) = I_c(T) \times \begin{cases} \frac{\sin\left(\frac{\pi H_{eff}(H_m, T, t)}{H_0(T)}\right)}{\left(\frac{\pi H_{eff}(H_m, T, t)}{H_0(T)}\right)} & \text{if } H_{eff} \leq \frac{H_0}{2}, \end{cases} \quad (1)$$

$$I_c(H_m, T, t) = I_c(T) \frac{H_0(T)}{\pi H_{eff}(H_m, T, t)} \quad \text{if } H_{eff} > \frac{H_0}{2}, \quad (2)$$

where *H<sub>0</sub>* is the effective field value at which the first minimum appears in the critical current versus field “Fraunhofer” pattern of an average Josephson junction of the material,<sup>21</sup> *I<sub>c</sub>(T)* is the temperature-dependent transport criti-

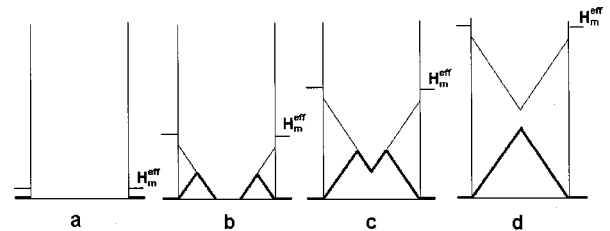


FIG. 1. Field profiles associated with a grain when the applied field reaches *H<sub>m</sub>* (thin lines) and when it is decreased to zero (bold lines). Four cases are represented as follows: (a) *H<sub>m</sub>*<sup>eff</sup> < *H<sub>c1g</sub>*(*T*), (b) *H<sub>c1g</sub>*(*T*) < *H<sub>m</sub>*<sup>eff</sup> < *H<sub>c1g</sub>*(*T*) + *H<sub>g</sub>*<sup>\*</sup>(*T*), (c) *H<sub>c1g</sub>*(*T*) + *H<sub>g</sub>*<sup>\*</sup>(*T*) < *H<sub>m</sub>*<sup>eff</sup> < *H<sub>c1g</sub>*(*T*) + 2*H<sub>g</sub>*<sup>\*</sup>(*T*), and (d) *H<sub>c1g</sub>*(*T*) + 2*H<sub>g</sub>*<sup>\*</sup>(*T*) < *H<sub>m</sub>*<sup>eff</sup>.

cal current at zero field, and  $H_{eff}$  is the effective intergranular field (described by different expressions, each one corresponding to a different magnetic field history of the sample). We have introduced the time dependence into the expressions through the time decay of the grains full penetration field, under the assumption that only the “outer” profiles of the grain magnetization as described by the critical state model contribute to the decay of  $H_{eff}$ . Below we present the four cases which are relevant to our experimental results (note that  $H_m^{eff}$  represents the average maximum effective field at the junctions).

(a) If  $H_m^{eff} < H_{c1g}(T)$  [Fig. 1(a)], then

$$H_{eff}(H_m, T, t) = 0. \quad (3)$$

(b) If  $H_{c1g}(T) < H_m^{eff} < H_{c1g}(T) + H_g^*(T)$  [Fig. 1(b)], then

$$H_{B1}(H_m, T) = -\frac{1-G}{G}H_g^*(T) + \sqrt{\left\{H_{c1g}(T) - \frac{1-G}{G}H_g^*(T)\right\}^2 + 2\frac{H_m}{G}H_g^*(T) - H_{c1g}^2(T)}. \quad (7)$$

(c) If  $H_{c1g}(T) + H_g^*(T) < H_m^{eff} < H_{c1g}(T) + 2H_g^*(T)$  [Fig. 1(c)], then

$$H_{eff}(H_m, T, t) = \frac{G}{1-G} \left\{ H_g^*(T) \delta_3 \left( \frac{\delta_3}{2} - 1 \right) + H_g^*(T, t) \times \left[ \frac{1}{2} + \delta_3 \left( \frac{\delta_3}{2} - 1 \right) \right] + H_{B2}(H_m, T) \delta_3 \right\}, \quad (8)$$

where

$$\delta_3 = 1 - \frac{H_{B2}(H_m, T)}{2H_g^*(T)}, \quad (9)$$

$$H_{B2}(H_m, T) = H_m + G \left\{ H_{c1g}(T) + \frac{1}{2}H_g^*(T) \right\} - H_{c1g}(T). \quad (10)$$

(d) If  $H_{c1g}(T) + 2H_g^*(T) < H_m^{eff}$  [Fig. 1(d)], then

$$H_{eff}(H_m, T, t) = \frac{G}{1-G} 2H_g^*(T, t). \quad (11)$$

In the above expressions,  $G$  is an averaged geometrical factor which depends on the microstructure of the sample with allowed values between 0 and 1. As mentioned before, we have assumed that flux creep affects the Bean’s full penetration field of the grains,  $H_g^*(T, t)$  [note that  $H_g^*(T)$  has been defined as  $H_g^*(T, t)$  evaluated at  $t = 10$  s]. This is a reasonable hypothesis, since, following Bean’s model,<sup>20</sup>  $H_g^*(T, t)$  is proportional to the magnitude of the bulk diamagnetic critical current responsible for the magnetization of a grain, which is supposed to decay due to thermal activation. In view of the inability of the original Anderson-Kim

$$H_{eff}(H_m, T, t) = \frac{G}{1-G} H_g^*(T) \left[ \delta_1 \left( \frac{\delta_1}{2} - 1 \right) - \delta_2 \left( \frac{\delta_2}{2} - 1 \right) \right] + \frac{G}{1-G} \left\{ H_g^*(T, t) \left[ \frac{1}{2} + \delta_1 \left( \frac{\delta_1}{2} - 1 \right) \right] + \frac{H_{B1}^2(H_m, T)}{2H_g^*(T)} \right\}, \quad (4)$$

where

$$\delta_1 = 1 - \frac{H_{B1}(H_m, T)}{2H_g^*(T)}, \quad (5)$$

$$\delta_2 = 1 - \frac{H_{B1}(H_m, T)}{H_g^*(T)}, \quad (6)$$

and

model<sup>22,23</sup> for explaining a number of features of flux creep in high- $T_c$  superconductors, we used the following expression based in the so-called *interpolation formula*:<sup>12</sup>

$$H_g^*(T, t) = H_g^*(0) \left\{ 1 + \mu \frac{k_B T}{U_0} \ln \left( \frac{t}{\tau} \right) \right\}^{-1/\mu}, \quad (12)$$

where  $H_g^*(0)$  is the average full penetration field of the grains at the initial instant and  $T = 0$ ,  $k_B$  is Boltzmann’s constant,  $U_0$  is the pinning energy of the grains,  $\tau$  is a characteristic time of the order of  $10^{-6}$  s (see, for example, Ref. 3), and  $\mu$  ranges from  $\frac{1}{7}$  to  $\frac{7}{4}$ , depending on the dimensionality of the pinning and creep regimes.<sup>24,25</sup> We have dismissed the possibility of flux creep effects on other parameters such as  $H_{c1g}$ , for example.

The combination of formulas (1) and (2) with (3)–(12) gives us the temporal dependence of the critical current density for a polycrystalline material. It should be noted that our approach accounts not only for the “usual” magnetic field history represented by formula (11) —i.e., that producing maximum (saturated) trapped field— but for the case of non-saturated remanent magnetization of the grains. The complexity of these situations is remarked upon by Yeshurum *et al.*,<sup>26</sup> and has attracted the attention of different authors,<sup>27–36</sup> but only in connection with magnetization measurements. To our knowledge, only Ref. 9 shows some experimental results associated with voltage relaxation in the presence of a transport current with different amounts of trapped magnetic field. It is worth noting that, although statistical distributions of the various parameters involved (such as  $H_0$  and  $G$ ) are usually considered in the literature<sup>17–19,21</sup> instead of the simple formulas (1) and (2), we avoided such a complication after checking that we were able to obtain

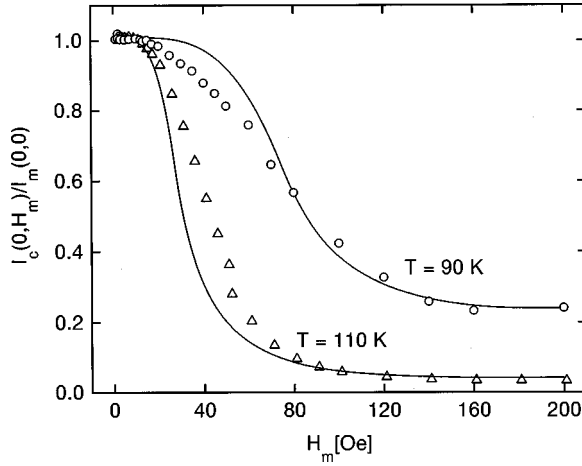


FIG. 2. Flux trapping characteristics at  $T=90$  K (circles) and  $T=110$  K (triangles) for the HBCCO sample. The solid lines follow the phenomenological model explained in the text.

similar results with or without statistical distributions, if our “effective,” parameters were appropriately chosen.

Let us now describe *grosso modo* how we proceeded for evaluating our phenomenological model. We first selected a set of parameters (not far from those expected for high- $T_c$  superconductors) for generating the transport flux trapping curve. After a few trials involving the tuning of the parameters, we obtained a reasonably good coincidence between theory and experiment, which gave us the “definitive” set of parameters. Then, we generated theoretical relaxation curves *with the same set of parameters* and compared their relaxations rates with those derived from the experiment. We assessed the validity of our phenomenological model by evaluating our ability to predict the field- and temperature-dependent experimental relaxations of the transport critical current. Each calculation for a given set of parameters involved the selection of the appropriate expressions through a simple program which followed the different scenarios defined earlier in this section. The details of this general procedure are described in the next section.

#### IV. RESULTS AND DISCUSSION

The circles and triangles in Fig. 2 show the flux trapping curve measured on sample  $(\text{Hg}_{1-x}\text{Re}_x)\text{Ba}_2\text{Ca}_2\text{Cu}_3\text{O}_{8+\delta}$  with  $x=0.24$  at  $T=90$  and  $110$  K normalized to their transport critical currents at  $H_m=0$ , respectively. Although this curve can give directly useful estimates for some intragranular parameters,<sup>15</sup> rigorous calculations of such parameters from the flux trapping curves require a fitting using formulas (1)–(12). This procedure has been used for the determination of the temperature dependences of  $H_{c1g}$ ,  $H_g^*$ , and  $H_0$  from the transport flux trapping curve (without consideration of any time dependence) by Muné *et al.*<sup>37</sup> The solid lines shown in Fig. 2 represent the result of substituting in formulas (1)–(12),  $G=0.25$ ,  $\mu=1$ ,  $U=0.4$  eV, and  $H_g^*(0)=120$  Oe, and assuming the following linear temperature dependences for  $H_{c1g}$  and  $H_0$  within the interval 90–110 K:

$$H_{c1g}(T) = H_{c1g}(0) \left( 1 - \frac{T}{T_{c1}} \right), \quad (13)$$

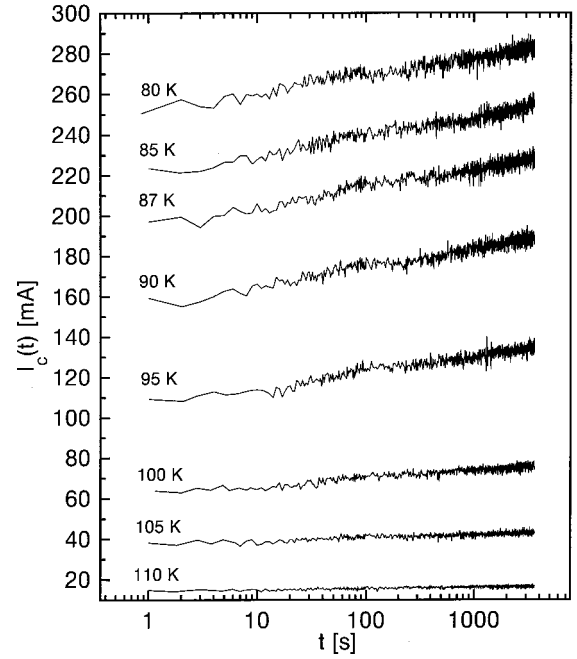


FIG. 3. Time evolution of the critical current measured at different temperatures and  $H_m=200$  Oe for the HBCCO sample.

$$H_0(T) = H_0(0) \left( 1 - \frac{T}{T_{c1}} \right), \quad (14)$$

where  $H_{c1g}(0)=20$  Oe,  $H_0(0)=57$  Oe, and  $T_{c1}=114$  K. Note that Eq. (14) is not the temperature dependence that would be expected by assuming the inverse proportionality of  $H_0(T)$  with the London penetration depth of the grains, as proposed by Peterson and Ekin.<sup>17</sup> Some of these parameters are reported by Reissner<sup>6</sup> from other experiments, and roughly match ours. The rest of our parameters are within the range commonly reported for other high- $T_c$  materials.<sup>15,18,37</sup> Finally, since each point of the flux trapping curve is measured after a few seconds of the establishment of the flux profile on the grains, formula (12) was evaluated at  $t=10$  s in order to resemble the experimental conditions. This time choice demonstrated only a small influence in the shape of the theoretical curves if moved within the 1–100 s interval. To summarize, *the only difference between the two theoretical curves showed in Fig. 2 is that they were generated for temperatures of 90 and 110 K, respectively.* As reported earlier for YBCO (Ref. 19) and BSSCO (Ref. 37) samples, the model reproduces quite well the features of the flux trapping curves, particularly at the two plateaus.

While a relatively fine tuning of the parameters  $G$ ,  $H_g^*(0)$ ,  $H_0(0)$  and  $T_{c1}$  was essential for the reproduction of the experimental flux trapping curves, the values of  $H_{c1g}(0)$ ,  $U_0$ , and  $\mu$  proved to be less influential. A good selection of  $U_0$  was important to reproduce the relaxation experiments, as discussed below. The value of  $\mu$  demonstrated a small influence on the fitting of the relaxation rates, so we just assigned  $\mu=1$ , which is close to the average value predicted for the different flux creep regimes mentioned earlier.

Figure 3 shows the transport critical current relaxation curves measured at different temperatures with  $H_m=200$  Oe.

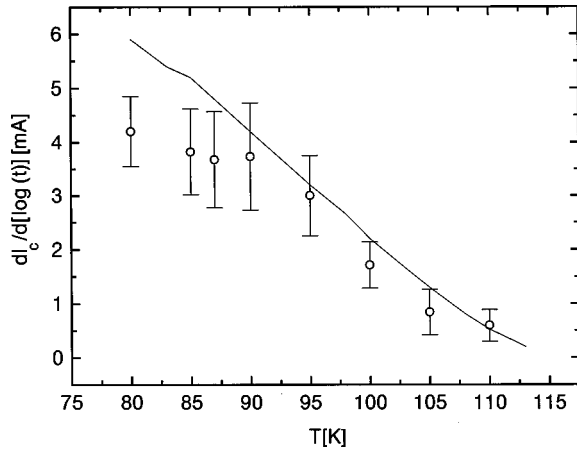


FIG. 4. Absolute relaxation rates of the transport critical current for different temperatures at  $H_m = 200$  Oe as derived from the experiment (circles) on the HBCCO sample. The solid line follows the phenomenological model described in the text.

Note the nearly logarithmic evolution of the critical current and the positive slope in all cases, which suggests that the effective field at the junctions decreases as the grains magnetizations relax, resulting in an increase of the transport critical current. The spots in Fig. 4 display the temperature dependance of the absolute relaxation rates defined as  $S = d(I_c)/d(\log t)$  which were extracted from the curves displayed in Fig. 3 (normalized relaxation rates were systematically avoided for the presentation of the experimental data<sup>3</sup>). The decrease of  $S$  with increasing temperature near  $T_c$  is a result observed by others in the case of magnetization measurements performed on high- $T_c$  films and crystals,<sup>3</sup> and, particularly, on HBCCO polycrystals,<sup>6</sup> but it is reported here for the relaxation of the transport critical current density. The solid curve in Fig. 4 is the result of our phenomenological model. It was generated by calculating the critical current versus time dependences from 1 to 3600 s at each temperature (all of which proved to be practically logarithmic), and then calculating their slopes from a semilogarithmic plot. To generate these curves the parameters  $G$ ,  $\mu$ ,  $U_0$ ,  $H^*(0)$ ,  $H_{c1g}(0)$ , and  $H_0(0)$  were the same as those used in the reproduction of the flux trapping characteristics. To calculate the absolute relaxation rates it was necessary to introduce the temperature dependence of the critical current density in formulas (1) and (2). It was obtained by fitting the experimental curve (not shown here) by the expression

$$I_c(T) = I_c(0) \left( 1 - \frac{T}{T_{c2}} \right)^{0.75}. \quad (15)$$

In Eq. (15),  $I_c(0) = 1600$  mA and  $T_{c2} = 122$  K. The ‘‘tail’’ of the experimental curve above 123 K was not considered in our fit.

Our model clearly reproduces the experimental behavior in the interval from 90 to 110 K, i.e., where the linear approximations (13) and (14) based on the flux trapping curves measured at 90 and 110 K, respectively, are reasonably good. Considering the work of Muné *et al.*<sup>37</sup> there are good reasons to believe that the linear approximations (13) and

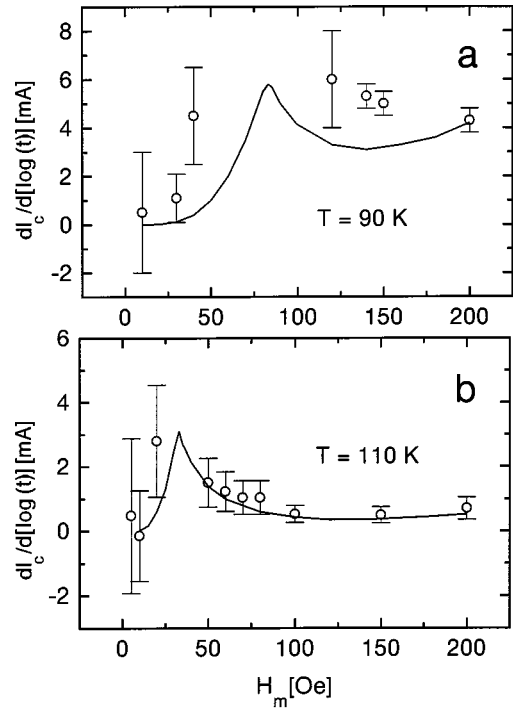


FIG. 5. Absolute relaxation rates of the transport critical current measured at  $T = 90$  K (a) and  $T = 110$  K (b) as a function of  $H_m$  for the HBCCO sample. The solid lines follow the phenomenological model described in the text.

(14) are not good below 90 K, which may explain the departure of our calculations from the experiment in that region, as observed in Fig. 4.

The time dependences of the critical current densities for different values of  $H_m$  (not shown here) displayed again a reasonably logarithmic behavior within our time window.

The circles in Fig. 5 correspond to the maximum applied field dependences of the transport critical current absolute relaxation rates at 90 K (a) and 110 K (b). Their most prominent feature is the existence of maxima located between 50 and 100 Oe at  $T = 90$  K, and between 25 and 50 Oe at  $T = 110$  K. This contrasts with many magnetic relaxation experiments found in the literature (at least in the same range of fields), where the relaxation rate increases from zero until it saturates roughly at the same  $H_m$  at which the magnetization versus  $H_m$  characteristic does.<sup>28,29</sup> However, maxima in the relaxation of the magnetic moment have been reported by Norling *et al.*<sup>33</sup> for YBCO polycrystals and by Blinov *et al.*<sup>35</sup> for YBCO films. It is our opinion that the existence of such maxima in the relaxation rates of the transport critical current of high- $T_c$  polycrystals is a result of potential technological relevance.

The solid lines in Fig. 5 correspond to the result of the application of our phenomenological model. They were generated by calculating the critical current versus time dependences from 1 to 3600 s at each field for a given temperature, and then determining their slopes from a semilogarithmic plot. To generate these curves the parameters  $G$ ,  $\mu$ ,  $U_0$ ,  $H^*(0)$ ,  $H_{c1g}(0)$ , and  $H_0(0)$  were the same as those used in the reproduction of the flux trapping characteristics. As stated earlier,  $U_0$  proved to be relevant for the reproduction of the experimental rates. The value of 0.4 eV is roughly

coherent with the results reported in Ref. 6 for HBCCO polycrystals, while it is an order of magnitude smaller than the values reported in Ref. 38 for the intergranular region of the same material. Although our theoretical curves seem to fit quite well the experimental data, it was impossible to obtain repetitive relaxation curves in the field regions at which the peaks predicted by the model were located.

As stated in the Experiment section, results qualitatively similar to those presented here have been obtained by us for a  $(\text{Hg}_{1-x}\text{Re}_x)\text{Ba}_2\text{Ca}_2\text{Cu}_3\text{O}_{8+\delta}$  sample with  $x=0.19$ . This is not surprising in the light of an energy-dispersive x-ray (EDX) analysis of Re-doped HBCCO polycrystals by Reder *et al.*,<sup>39</sup> which shows that the intragranular defect structure of their samples does not change with Re content.

The lack of data for a complete comparison between experiment and theory relative to the  $H_m$  dependence of the relaxation rate in HBCCO ceramics made us try a different system, i.e., a YBCO polycrystal. The measurement process was identical to the one earlier performed on the HSCCO system, as well as the steps for the selection of parameters in the phenomenological model. We only show here, for brevity's sake, the temperature and remanent field dependences of the absolute relaxation rates of the transport critical current for the YBCO sample. Our choice of parameters was  $G=0.25$ ,  $\mu=1$ ,  $U_0=0.6$  eV,  $H^*(0)=90$  Oe,  $H_{c1g}(0)=45$  Oe,  $H_0(0)=30$  Oe,  $I_c(0)=8055$  mA, and  $T_{c1}=T_{c2}=88$  K. Most of these parameters are coherent with those reported in the literature for YBCO polycrystals,<sup>15,9,18</sup> while  $\mu=1$  was selected following the same reasoning as for the HBCCO sample. As expected, our choice for  $U_0$  is an order of magnitude smaller than the intergranular pinning energy reported in Ref. 31 for YBCO polycrystals.

Before presenting the results, a few features of the curves not shown here for the YBCO system should be stated: (a) the flux trapping curves were better matched by our model than in the case of HSCCO, (b) the temperature dependence of the transport critical current was fitted by

$$I_c(T) = I_c(0) \left( 1 - \frac{T}{T_{c2}} \right) \quad (16)$$

instead of Eq. (15), and (c) the time evolution of the critical current was nearly logarithmic for our time, temperature, and trapped field windows, as in the case of the HBCCO system.

The circles in Fig. 6 display the experimental values of the critical current relaxation rates as  $T$  increases for  $H_m=160$  Oe in the case of YBCO, while the solid line resulted from introducing in our phenomenological model the parameters given above. In Fig. 7, the  $H_m$  dependence of the critical current relaxation rates is displayed by open circles for 80 K (a) and 85 K (b). When these results are compared with the analogous ones for the HBCCO system, a general pattern emerges: as  $T$  increases, the experimental maxima shift to lower values of  $H_m$ , decrease their intensity, and sharpen. The theoretical fits (shown as solid lines) appropriately reproduce the position of the peaks, but their intensities and widths are not perfectly reproduced. In principle, several additions may be introduced in our model to improve these results. Two of the most straightforward ones are the recognition that  $\mu$  is a function of temperature and that the pinning

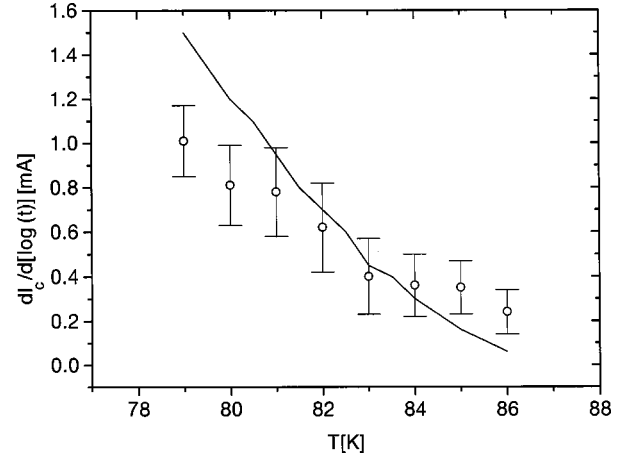


FIG. 6. Absolute relaxation rates of the transport critical current for different temperatures at  $H_m=160$  Oe as derived from the experiment (circles) for the YBCO sample. The solid line follows the phenomenological model described in the text.

energy may depend on the magnetic field. A less trivial improvement would be to introduce the percolative character of the transport current, which has improved the fits of flux trapping curves performed by Muné and López.<sup>40</sup> These modifications, however, would introduce some additional parameters in the model, and are beyond the scope of the present work.

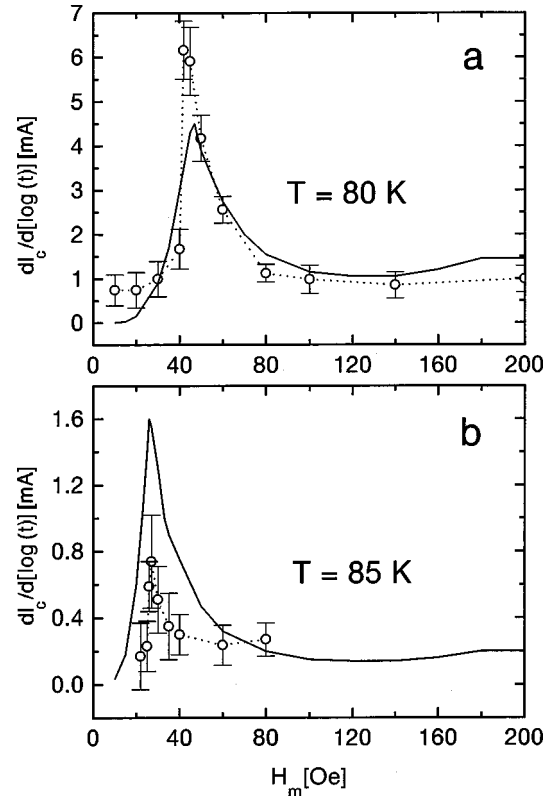


FIG. 7. Absolute relaxation rates of the transport critical current measured at  $T=80$  K (a) and  $T=85$  K (b) as a function of  $H_m$  for the YBCO sample. The dotted lines connect experimental points, while the solid lines follow the phenomenological model described in the text.

## V. CONCLUSION

We have performed a systematic experimental study of the time relaxation of the critical current density of  $(\text{Hg}_{1-x}\text{Re}_x)\text{Ba}_2\text{Ca}_2\text{Cu}_3\text{O}_{8+\delta}$  and  $\text{YBa}_2\text{Cu}_3\text{O}_{7-\delta}$  polycrystals by means of 1-h runs covering a range of temperatures from 80 to 110 K and remanent magnetic fields resulting from ZFC excursions to maximum applied fields ranging from 0 to 200 Oe.

Within our time, temperature, and remanent field windows, the transport critical currents increased logarithmically in time. The absolute relaxation rates decreased with increasing temperature, while they showed a peak when plotted as a function of the maximum applied field  $H_m$ . The position of the peak shifts to smaller values of  $H_m$  as the temperature approaches  $T_c$ , and its width and intensity decrease.

To interpret the experimental results, we propose a phenomenological model which holds, in principle, for any

polycrystalline superconductor. It considers the effect of the intragrain flux creep at the intergrain junctions, which affects the transport current. Despite our model reproducing quite well our experimental results, it seems necessary to improve it by taking into account the percolative nature of the transport current and the temperature and field dependences of some parameters related to the thermally activated processes involved.

## ACKNOWLEDGMENTS

We would like to thank the useful comments of L. Civale, R. Mulet and J.L. González. This work was partially supported by TWAS Grant No. 95-124 RG/PHYS/LA and by the University of Havana's "Alma Mater" program. M.T.D.O. acknowledges financial support from CNPq, FINEP, CAPES, CST, CVD, and UFES.

- <sup>1</sup>J.G. Bednorz and K.H. Müller, *Z. Phys. B* **64**, 189 (1986).
- <sup>2</sup>Y. Yeshurun and A.P. Malozemoff, *Phys. Rev. Lett.* **60**, 2202 (1988).
- <sup>3</sup>Y. Yeshurun, A.P. Malozemoff, and A. Shaulov, *Rev. Mod. Phys.* **68**, 911 (1996).
- <sup>4</sup>See, for example, M. Xu, D. Shi, A. Umezawa, K.G. Van der Voort, and G.W. Crabtree, *Phys. Rev. B* **43**, 13 049 (1991).
- <sup>5</sup>See, for example, Q. Hong and J.H. Wang, *Physica C* **257**, 367 (1996).
- <sup>6</sup>M. Reissner, *Physica C* **290**, 173 (1997).
- <sup>7</sup>D.N. Matthews, G.J. Russell, and K.N.R. Taylor, *Physica C* **171**, 301 (1990).
- <sup>8</sup>J. Wang, K.N.R. Taylor, D.N. Matthews, H.K. Liu, G.J. Russell, and S.X. Dou, *Physica C* **180**, 307 (1991).
- <sup>9</sup>E. Altshuler and J.L. González, *Physica C* **200**, 195 (1992).
- <sup>10</sup>A.A. Zhukov, D.A. Komarkov, G. Karapetov, S.N. Gordeev, and R.I. Antonov, *Supercond. Sci. Technol.* **5**, 338 (1992).
- <sup>11</sup>G. Ries, H.W. Neumüller, W. Schmidt, and C. Struller (unpublished).
- <sup>12</sup>G. Blatter, M.V. Feigel'man, V.B. Geshkenbein, A.I. Larkin, and V.M. Vinokur, *Rev. Mod. Phys.* **66**, 1125 (1994).
- <sup>13</sup>A. Sin, A.G. Cunha, A. Calleja, M.T.D. Orlando, F.G. Emmerich, E. Baggio-Saitovich, M. Segarra, S. Piñol, and X. Obradors, *Adv. Mater.* **10**, 1126 (1998).
- <sup>14</sup>A. Sin, A.G. Cunha, A. Calleja, M.T.D. Orlando, F.G. Emmerich, E. Baggio-Saitovich, S. Piñol, J.M. Chimens, and X. Obradors, *Physica C* **306**, 34 (1998).
- <sup>15</sup>E. Altshuler, S. García, and J. Barroso, *Physica C* **177**, 61 (1991).
- <sup>16</sup>L.E. Flores and C. Martínez, *Cryogenics* **36**, 705 (1996).
- <sup>17</sup>R.L. Peterson and J.W. Ekin, *Phys. Rev. B* **37**, 9848 (1988).
- <sup>18</sup>E. Altshuler, J. Musa, J. Barroso, A.R.R. Papa, and V. Venegas, *Cryogenics* **33**, 308 (1993).
- <sup>19</sup>K.H. Müller and D.N. Matthews, *Physica C* **206**, 275 (1993).
- <sup>20</sup>Ch. Bean, *Rev. Mod. Phys.* **30**, 31 (1964).
- <sup>21</sup>A.R.R. Papa and E. Altshuler, *Solid State Commun.* **76**, 799 (1990).
- <sup>22</sup>P.W. Anderson, *Phys. Rev. Lett.* **9**, 309 (1962).
- <sup>23</sup>P.W. Anderson and Y.B. Kim, *Rev. Mod. Phys.* **36**, 39 (1964).
- <sup>24</sup>M.V. Feigel'man, V.B. Geshkenbein, A.I. Larkin, and V.M. Vinokur, *Phys. Rev. Lett.* **63**, 2303 (1989).
- <sup>25</sup>V.M. Vinokur, P.H. Kes, and A.E. Koshelev, *Physica C* **168**, 29 (1990).
- <sup>26</sup>Y. Yeshurun, A.P. Malozemoff, and F. Holtzberg, *J. Appl. Phys.* **64**, 5797 (1988).
- <sup>27</sup>A.C. Mota, A. Pollini, P. Visani, K.H. Müller, and J.G. Bednorz, *Physica C* **153-155**, 67 (1988).
- <sup>28</sup>A.C. Mota, P. Visani, and A. Pollini, *Physica C* **153-155**, 441 (1988).
- <sup>29</sup>A.C. Mota, G. Juri, P. Visani, and A. Pollini, *Physica C* **162-164**, 1152 (1989).
- <sup>30</sup>K. Kwasnitza and Ch. Widmer, *Physica C* **184**, 341 (1991).
- <sup>31</sup>E.V. Blinov, E. Lähderanta, R. Laiho, and Yu. Stephanov, *Physica C* **199**, 201 (1992).
- <sup>32</sup>R. Mulet, L. Flores, and E. Altshuler, *Phys. Status Solidi B* **182**, K31 (1994).
- <sup>33</sup>P. Norling, K. Niskanen, J. Magnusson, P. Nordblad, and P. Svédlinde, *Physica C* **221**, 169 (1994).
- <sup>34</sup>E.V. Blinov, R. Laiho, E. Lähderanta, Yu. Stephanov, and K. Traito, *Phys. Rev. B* **51**, 3824 (1995).
- <sup>35</sup>E.V. Blinov, R. Laiho, E. Lähderanta, A.G. Lyublinsky, and K.B. Traito, *Physica C* **269**, 268 (1996).
- <sup>36</sup>M.A.R. LeBlanc, D.S.M. Cameron, S. Celebi, and J.P. Pascal, *Supercond. Sci. Technol.* **11**, 359 (1998).
- <sup>37</sup>P. Muné, J. López, and E. Altshuler, *Physica C* **292**, 48 (1997).
- <sup>38</sup>G.C. Kim, M.Y. Cheon, and Y.C. Kim, *Physica C* **300**, 105 (1998).
- <sup>39</sup>M. Reder, J. Krelaus, K. Heinemann, H.C. Freyhardt, F. Ladenberger, and E. Schwarzmann *Applied Superconductivity 1997*, Proceedings of the EUCAS 1997, Netherlands, 1997, IOP Conf. Proc. No. 158, edited by H. Rogalla and D.H.A. Blank (Institute of Physics, London, 1997), Vol. 2, pp. 933–936.
- <sup>40</sup>P. Muné and J. López, *Physica C* **257**, 360 (1996).